REPORT

Somatic Mutations in *NEK9* Cause Nevus Comedonicus

Jonathan L. Levinsohn,[1,2] Jeffrey L. Sugarman,[3] Yale Center for Mendelian Genomics, Jennifer M. McNiff,[2,4] Richard J. Antaya,[2,5] and Keith A. Choate[1,2,4,*]

Acne vulgaris (AV) affects most adolescents, and of those affected, moderate to severe disease occurs in 20%. Comedones, follicular plugs consisting of desquamated keratinocytes and sebum, are central to its pathogenesis. Despite high heritability in first-degree relatives, AV genetic determinants remain incompletely understood. We therefore employed whole-exome sequencing (WES) in nevus comedonicus (NC), a rare disorder that features comedones and inflammatory acne cysts in localized, linear configurations. WES identified somatic *NEK9* mutations, each affecting highly conserved residues within its kinase or RCC1 domains, in affected tissue of three out of three NC-affected subjects. All mutations are gain of function, resulting in increased phosphorylation at Thr210, a hallmark of NEK9 kinase activation. We found that comedo formation in NC is marked by loss of follicular differentiation markers, expansion of keratin-15-positive cells from localization within the bulge to the entire sub-bulge follicle and cyst, and ectopic expression of keratin 10, a marker of interfollicular differentiation not present in normal follicles. These findings suggest that *NEK9* mutations in NC disrupt normal follicular differentiation and identify *NEK9* as a potential regulator of follicular homeostasis.

Acne vulgaris (AV) is a common disorder affecting nearly all adolescents, and it can range in severity from isolated non-inflammatory open and closed comedones to raised inflammatory lesions and pustules.[1] The most severe cases demonstrate nodulocystic inflammatory disease, and up to 20% of affected individuals experience permanent scarring.[2]

Microcomedones, which consist of plugs of desquamated keratinocytes, are thought to be precursors to acne lesions. These plugs trap sebum and keratin within follicles, leading to the formation of dilated plugged follicles known as comedones. The nutrient-rich environment within the comedo can lead to overgrowth of *P. acnes* and subsequent inflammation.[3] Current treatment for AV includes topical or systemic retinoids, antibiotics, and benzoyl peroxide. These agents are thought to prevent comedo formation and inflammation by promoting differentiation of cells within the hair follicle unit, reducing sebum secretion and sebocyte proliferation, and killing *P. acnes*.[4]

Genetic investigation of Mendelian acne phenotypes has identified pathways implicated both in the generation of comedones and in subsequent inflammatory responses. Apert syndrome (MIM: 101200), a rare congenital disease that presents with craniosynostosis, syndactyly, and severe acne with comedones and inflammatory cysts, is caused by heterozygous activating mutations in *FGFR2* (MIM: 176943).[5] Munro acne nevus is a localized form of Apert syndrome that results from somatic *FGFR2* mutation and features linear groups of comedones and inflammatory cysts.[6] These disorders suggest that FGFR2 signaling might be important both in comedogenesis and inflammation, and mouse models have shown that FGFR2 is necessary for skin and hair follicle homeostasis and regulation of cutaneous inflammation.[7,8]

Acne inversa (MIM: 42690), a heritable type of inflammatory acne found in axillary, inguinal, and perianal regions, presents with comedones, inflammatory nodules, and draining sinus tracts.[9] A subset of individuals with acne inversa have mutations in *PSENEN* (MIM: 607632), *PSEN1* (MIM: 104311), and *NCSTN* (MIM: 605254) which act within the γ-secretase pathway, implicating Notch signaling defects in comedogenesis.[10] Evidence in mouse models suggests that, as in *FGFR2* mutations, γ-secretase haploinsufficiency might promote comedo formation, leading to subsequent inflammation.[11]

Genome-wide association studies (GWASs) in AV have identified multiple loci associated with severe acne. A GWAS involving Chinese Han individuals found two loci, one near *DDB2* (MIM: 600811) and the other within *SELL* (MIM: 153240). These genes are thought to play a role in anti-microbial activity of sebocytes (*DDB2*) and mediation of cutaneous inflammation (*SELL*), respectively.[12] A GWAS involving European individuals found three separate loci, containing the genes *OVOL1* (MIM: 602313), *FST* (MIM: 136470), and *TGFB2* (MIM: 190220), all active in TGF-β signaling, which might modulate the inflammatory response to comedonal lesions or play a role in tissue remodeling.[13,14]

Nevus comedonicus (NC) is a severe, localized form of acne estimated to be present in 1:45,000–1:100,000 births and appears in infancy as a linear shiny patch with development of comedones early in life.[15] Some of these comedones can subsequently become inflamed and form acne cysts, suggesting that NC lesions result from a process that most directly leads to comedo development with inflammation occurring as a secondary consequence.[1] The linear configuration of NC lesions suggests that NC is a mosaic disorder resulting from

[1]Department of Genetics, Yale School of Medicine, New Haven, CT 06510, USA; [2]Department of Dermatology, Yale School of Medicine, New Haven, CT 06510, USA; [3]Departments of Dermatology and Family Medicine, University of California, San Francisco, San Francisco, CA 94143, USA; [4]Department of Pathology, Yale School of Medicine, New Haven, CT 06510, USA; [5]Department of Pediatrics, Yale School of Medicine, New Haven, CT 06510, USA
*Correspondence: keith.choate@yale.edu
http://dx.doi.org/10.1016/j.ajhg.2016.03.019.

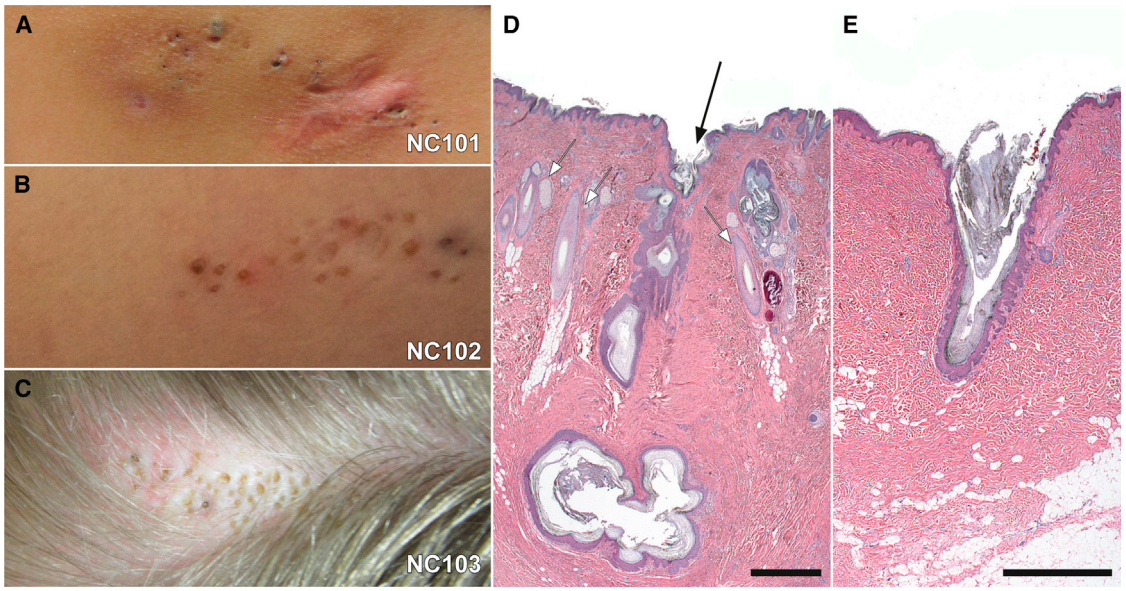

Figure 1. Clinical and Histologic Features of Nevus Comedonicus
Three unrelated subjects presented with linear patches of comedones on distinct body sites. NC101, a 43-year-old woman, had a lesion on the back that featured numerous dilated follicular ostia and comedones, with a scar inferiorly at the site of a prior inflammatory lesion (A). NC102, a 10-year-old boy, had a lesion on the thigh that featured numerous comedones and atrophic scars at the sites of prior inflammatory lesions (B). NC103, a 19-year-old woman, had a hairless patch on the scalp. The patch subsequently never grew hair and developed multiple comedones and inflammatory cysts (C). Intervening skin appeared grossly normal in all subjects. Histopathologic examination of affected scalp excision tissue in subject NC103 revealed normal hair follicles (white arrows) adjacent to affected follicles (black arrow), which show dilated follicular ostia, marked acanthosis and papllimatosis of the outer root sheath, and large cystic structures filled with keratin in the deep dermis (D). Examination of tissue excised from the back of subject NC101 shows an isolated follicle with a dilated ostium, acanthosis and papillomatosis of the outer root sheath, and accumulated keratin in place of a hair shaft (E). In both cases, interfollicular epidermis appears to be normal. Scale bars represent 1 mm.

acquisition of a somatic mutation during embryonic development.

In cutaneous mosaic disorders due to mutations within keratinocyte precursors, including NC, skin lesions are found in linear configurations known as lines of Blaschko, which represent the dorsoventral migration of epithelial progenitors.[16] When multilineage somatic mosaicism occurs, more widespread involvement is seen, as in the cutaneous-skeletal hypophosphatemic syndrome, which features hypophosphatemic rickets, epidermal and melanocytic nevi, and hamartomas in multiple organs as a result of multilineage somatic activating *RAS* mutations.[17] Extracutaneous manifestations have also been reported in individuals with NC, leading to the diagnosis of nevus comedonicus syndrome, which can feature NC lesions, ipsilateral cataracts, and neurological and skeletal abnormalities.[18]

To determine the genetic cause of NC, we recruited a cohort of three subjects with NC lesions, and consent to a protocol approved by the Yale University human investigation committee was obtained. All subjects had a history of localized linear lesions featuring intermixed non-inflammatory grouped comedones, scars, and recurrent inflammatory cysts without other intervening skin changes. Subjects provided a skin biopsy from lesional tissue and a peripheral blood sample for analysis.

NC101, a 43-year-old woman, initially presented with a 6 cm × 3 cm linear lesion consisting of grouped comedones on the back and a history of inflammatory cysts within the lesion (Figure 1). NC102, a 10-year-old boy, presented at birth with a shiny flat lesion on the right inferior buttock. At the age of 10 months, this lesion began to develop intermittent inflammatory cysts with cribriform scarring, and comedones became apparent. At the time of enrollment, this lesion extended inferiorly to the postero-medial right thigh and was a 10 cm × 2 cm plaque composed of several atrophic cribriform scars and scattered pink comedones that were surmounted by a thin scale crust. Inferior to this plaque was a second, similar appearing one measuring 2 cm × 1 cm (Figure 1). NC103, a 19-year-old woman, presented with a 1 cm × 4 cm lesion on the scalp that appeared at birth and subsequently developed alopecia, comedones, and rare inflammatory cysts (Figure 1).

Histopathology of the NC103 lesion revealed follicles with dilated ostia adjacent to normal follicles. These abnormal follicles demonstrated acanthosis and papillomatosis of the outer root sheath. Furthermore, large cystic structures filled with keratin were present in the deep dermis (Figure 1). Examination of tissue from NC101 showed isolated follicles with dilated ostia and acanthosis and papillomatosis of the outer root sheath. Accumulated keratin was present without evident hair shafts (Figure 1).

A

Sample	Position (hg19)	Gene	Base Change	Protein Effect	Reads tissue ref	Reads tissue nonref	Reads blood ref	Reads blood nonref	p value
NC101	chr14:75570544	***NEK9***	G>T	p.Gly572_Glu577del	153	29	91	0	4.3×10^{-6}
NC101	chr14:75570561	***NEK9***	G>T	p.Gly572_Glu577del	136	28	82	0	7.0×10^{-6}
NC102	chr14:75570558	***NEK9***	T>C	p.Ile573Thr	65	12	66	0	4.4×10^{-4}
NC103	chr14:75587237	***NEK9***	T>C	p.Ile167Thr	226	33	184	0	9.3×10^{-9}

B

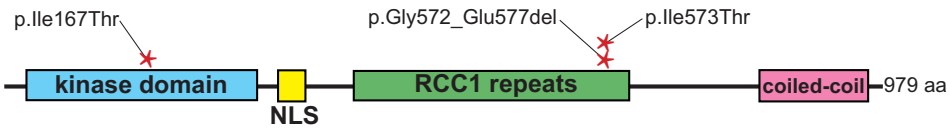

Figure 2. Somatic *NEK9* Mutations Cause Nevus Comedonicus
Whole-exome sequencing of DNA isolated from tissue and blood of individuals NC101, NC102, and NC103 was performed (A). Using MuTect, Perl and Python scripts, we identified tissue-specific SSNVs and indels and ranked them by Fisher's exact test score. NC101 had two mutations in *NEK9* that were in *cis* on spanning short reads. These mutations led to a loss of six amino acids in the encoded protein, p.Gly572_Glu577del, via abolition of the native exon 14 splice donor and utilization of a cryptic splice donor within the coding region of exon 14 (Figure S3). NC102 had a somatic *NEK9* p.Ile573Thr missense variant. NC103 showed a somatic NEK9 p.Ile167Thr missense variant. No other somatic mutations were found in any of the three individuals with a Fisher's exact test p value $< 1 \times 10^{-4}$, and no non-reference reads were identified in blood DNA in any individual. Mutations were confirmed with Sanger sequencing (Figure S2). NC101's and NC102's mutations were localized in the RCC1 domain of NEK9, whereas NC103's mutation was localized in the kinase domain (B).

In contrast to the smooth, ordered layer of keratinocytes seen in the outer root sheath of hair follicles, the acanthosis and papillomatosis of cells lining the NC follicle and cyst regions presented a morphology similar to rete ridges in interfollicular epidermis. Although lesional tissue was limited, NC comedonal follicles did not appear to have associated sebaceous lobules. Interfollicular skin in NC lesions was normal on clinical and histologic examination.

These clinical and histologic findings are distinct from Apert syndrome, Munro acne nevus, and acne inversa. The characteristic sinus tracts and double comedones of acne inversa were not observed in any NC lesions. Histologic findings further distinguish Apert syndrome and Munro acne nevus from NC, given that both demonstrate a flat, atrophic cyst wall and numerous associated sebaceous lobules, in contrast to the papillomatosis and acanthosis of the NC follicle and cyst, which also lack sebaceous lobules.[19]

We isolated DNA from blood and tissue samples by using a phenol-chloroform extraction or DNeasy (QIAGEN), respectively. Using paired samples from each of the three subjects, we performed whole-exome capture (Roche EZ exome V3) followed by high-throughput sequencing (Illumina HiSeq 2500), generating average coverage $> 90\times$ for tissue samples and $> 85\times$ for blood samples (Table S1). Sequence was aligned to the human genome reference (UCSC Genome Browser, hg19) with the Burrows-Wheeler Aligner (BWA-MEM).[20] Reads were then trimmed and PCR duplicates removed with Picard,[21] and resultant BAM files were calibrated with GATK.[21] To identify somatic single-nucleotide variants (SSNVs) present in tissue samples but absent in the matched blood sample, we employed MuTect[22] and a Fisher's exact test to compare blood and tissue read numbers; SSNVs with a p value greater than 1×10^{-3} were excluded. Remaining SSNVs were annotated with AnnoVar.[23] To exclude common and non-damaging variants, we further analyzed nonsynonymous exonic and splice-site SSNVs with a prevalence $< 1\%$ in an Exome Aggregation Consortium (ExAC) control dataset (Table S2). For each of the three paired samples, all of these high-confidence SSNVs identified were located within a single gene, *NEK9* (MIM: 609798), which encodes a kinase. These occurred at highly conserved residues, and none of the mutations were found in >134,000 alleles in ExAC, Exome Variant Server, and 1000 Genomes control databases. All were confirmed via Sanger sequencing (Figure S2). We found no evidence of loss of heterozygosity or genomic segment amplification or deletion (Figure 2 and Figure S1) in any sample.

To estimate the probability of observing three somatic mutations clustering within a 3 kb coding region (the size of *NEK9*) by chance, we performed a Monte Carlo simulation, counting the two mutations found in NC101 as a single genetic event. We distributed all three observed somatic mutations in the three samples across a 31 Mb coding region and determined the frequency with which three mutations clustered within a 3 kb segment. In 10^8 iterations of this simulation, we estimate the probability of observing a mutation in *NEK9* in all three samples to be approximately 6×10^{-8}.

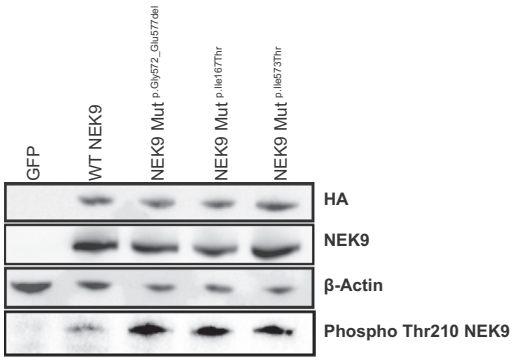

Figure 3. *NEK9* Mutations Cause Increased Phosphorylation of NEK9

HEK293 cells were transiently transfected with GFP as a negative control or HA-tagged *NEK9* constructs, including those encoding wild-type (WT) NEK9, p.Gly572_Glu577del NEK9, p.Ile167Thr NEK9, and p.Ile573Thr NEK9. 24 hr post-transfection with lipofectamine 2000 (Invitrogen), protein lysates were run on SDS-page gels and transferred to nitrocellulose. Blots were probed with 1:1,000 anti-HA (ab18181; Abcam), 1:1,000 anti-beta-actin (A5316; Sigma), 1:10,000 anti-NEK9 (ab138488; Abcam), and 1:250 anti-phospho-NEK9 (ab63553; Abcam). In contrast to expression of wild-type NEK9, expression of each of the three mutant constructs led to increased phosphorylation of NEK9 despite equivalent protein expression detected by blotting for HA, total NEK9, and actin. This experiment was repeated three times, confirming increased phospho-NEK9 in cells expressing mutant alleles.

This analysis revealed two somatic *NEK9* mutations in *cis* in individual NC101: c.1731+1G>T (GenBank: NM_033116.4), which abolishes a native splice donor, at the exon 14 and intron 14 junction and c.1715G>T (p.Gly572Val), which generates a cryptic splice donor site, within exon 14 (Figure 2). To assess mutation consequence, we cloned a segment containing exons 13 to 15 of wild-type and mutant (c.1715G>T and c.1731+1G>T) *NEK9* into pcDNA3.1. Resulting constructs were transfected into PLC cells, and we performed RT-PCR 48 hr after transfection, using RNeasy (QIAGEN) for RNA isolation and iScript (BD Biosciences) for cDNA generation. PCR was then used to amplify exons 13 to 15, and products were Sanger sequenced. This assay demonstrated loss of 18 nucleotides in the encoded mRNA (p.Gly572_Glu577del), corresponding to deletion of amino acids 572–577 (Figure S3). All six of these amino acids are highly conserved, demonstrating conservation in 100%, 93%, 84%, 100%, 99%, and 89% of 100 vertebrates, respectively (Figure S4).

Individual NC102 had a single somatic missense mutation (c.1718T>C [p.Ile573Thr]) in exon 14 of *NEK9*, affecting one of the amino acids that we found deleted in NC101. The isoleucine in this position is conserved in 93% of vertebrates, and no species demonstrates a threonine at this position. The affected amino acids in NC101 and NC102 fall within the regulator of chromosome condensation-like (RCC1) domain of NEK9 (Figure 2). Previous reports have shown that deletion of the NEK9 RCC1 domain causes increased kinase activity via autophosphorylation, suggesting that the observed mutations might abrogate RCC1-mediated suppression of NEK9 kinase activity.[24]

In individual NC103, we found a somatic mutation (c.500T>C [p.Ile167Thr]) in exon 4 of *NEK9*, which occurs in the kinase domain of the protein (Figure 2). This isoleucine residue is 100% conserved in vertebrates (Figure S4). There is in vitro evidence that the NEK9 kinase and RCC1 domains bind to each other,[24] potentially linking the NC101 and NC102 mutations within the RCC1 domain to the kinase-domain mutation in NC103.

NEK9 is a serine/threonine kinase that functions as an important regulator of cell-cycle and checkpoint control and is a member of a larger family of NEK proteins that share moderate conservation.[24] Phosphorylation by PLK1 and CDK1 at Ser29, Thr333, Ser750, and Ser869 are required steps for activation of NEK9 and precede phosphorylation at Thr210, which can also occur autocatalytically or via PLK1 action.[25] Thr210 lies within the activation loop of NEK9, and phosphorylation at this residue is required for kinase activity.[25]

The finding of somatic *NEK9* mutations within affected tissue of three NC-affected subjects is consistent with either a gain-of-function or a dominant-negative mechanism. To study the effect of these mutations, we obtained the *NEK9* cDNA (Harvard Plasmid) and introduced the observed mutations via QuikChange Site-Directed Mutagenesis (Agilent). An HA tag was introduced at the N terminus via PCR, and tagged wild-type and mutant constructs were transfected into pCAGGS via Gibson assembly (New England Biolabs). We transiently transfected resulting cDNAs of wild-type NEK9 and mutants into HEK293 cells and assayed levels of Thr210-phosphorylated NEK9 by western blotting. We found that, relative to wild-type, all three NC mutations significantly increased NEK9 Thr210 phosphorylation (Figure 3). Given prior observations that Thr210 phosphorylation is necessary for NEK9 kinase activity, and that NEK9 auto-phosphorylation increases kinase activity,[25] our data support the hypothesis that NC mutations are gain of function.

Given the presence of independent somatic mutations in affected tissue of three subjects with NC, including one lesion with comedones replacing hair follicles on the scalp (Figure 1), we sought to investigate localization of NEK9 in hair-bearing skin. Within normal skin, immunolocalization studies showed NEK9 localized to the epidermis and hair follicles. In both interfollicular epidermis and in affected dilated follicles of NC tissue, we found no change in subcellular localization in comparison to normal tissue (Figure S5). To further explore the consequences of *NEK9* mutation, we performed immunolocalization studies employing hair follicle and epidermal differentiation markers in NC lesional tissue and a normal control after antigen retrieval (incubation in 10 mM sodium citrate, 0.05% Tween 20 [pH 6.0] at 100°C for 20 min). We found abnormal localization of multiple markers of hair follicle and epidermal differentiation (Figure 4). Expansion of keratin 15 (K15) immunostaining

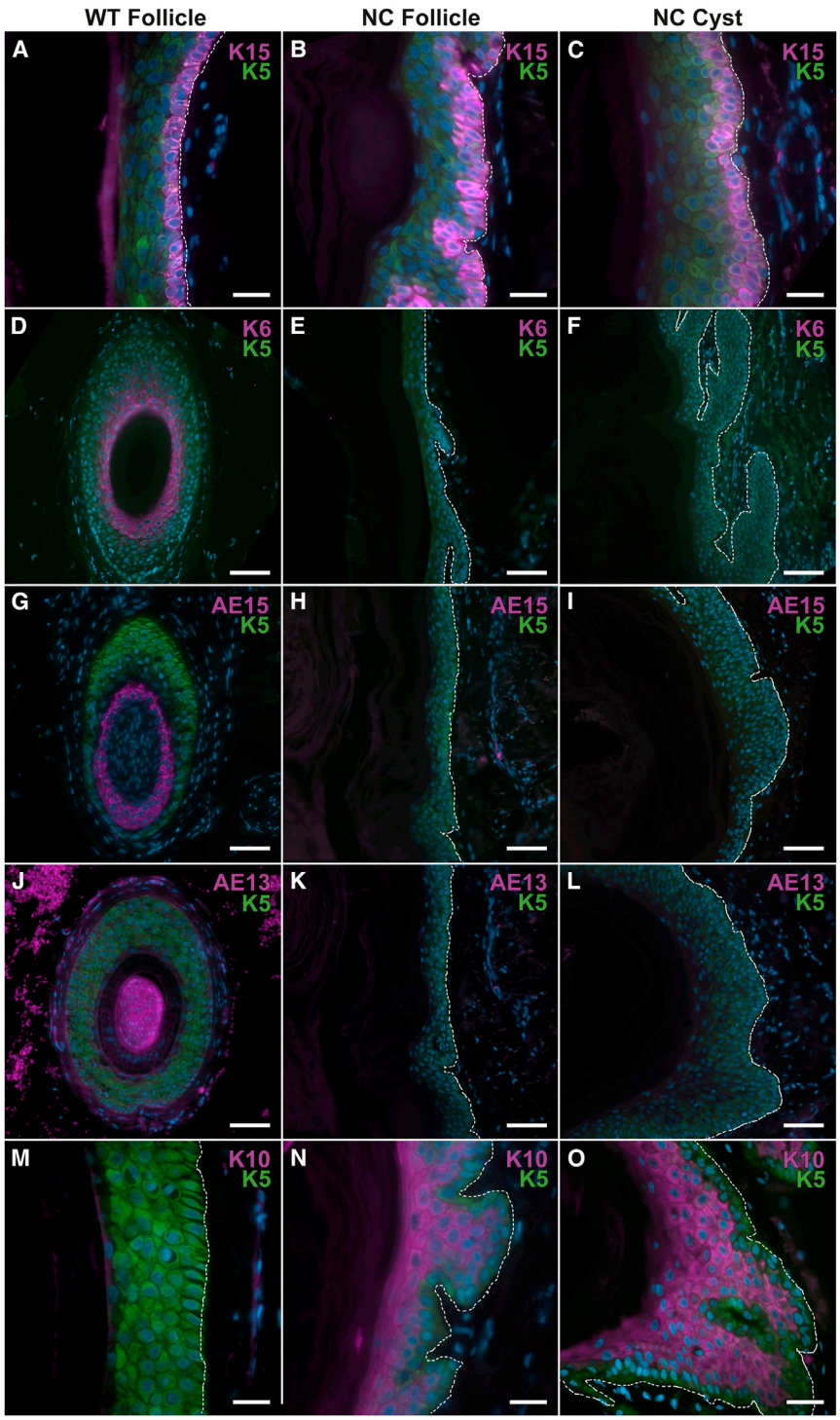

Figure 4. *NEK9* Mutation Impairs Follicular Differentiation

In NC103 lesional tissue, follicular differentiation was analyzed by immunofluorescence staining. Keratin 5 staining in all images marks the outer root sheath of the hair follicle. To characterize the stem cell pool in NC, staining for keratin 15 (K15) was performed. K15 localizes to the basal layer of keratinocytes within the bulge in normal hair follicles (A), but in NC was found to strongly localize to the basal layer throughout the follicle (B) and cyst (C). In normal tissue, keratin 6, AE15 and AE13 mark follicular differentiation in the companion layer, inner root sheath, and cuticle and cortex, respectively (D, G, and J). In NC, these were absent in the upper follicular regions (E, H, and K), as well as within cysts (F, I, and L), suggesting a shift in follicular fate to an IFE-like fate within NC tissue. To further assess differentiation of follicular cells, keratin 10 (K10) staining was examined. K10, a marker of suprabasal IFE, which is absent in sub-bulge regions of normal follicles (M), was found within the upper follicular and sub-bulge region of NC (N) and within the cysts of NC tissue (O), in both cases maintaining suprabasal localization. The dermal-epidermal junction is labeled with a dashed white line in each panel. Control tissue was obtained from discarded tips from surgical excision. Scale bar represents 20 μm in (A)–(C) and (M)–(O) and 50 μm in (D)–(L).

(sc-47697, dilution 1:200; Santa Cruz), a marker of the hair follicle bulge, which is thought to be the location of the hair follicle stem cell pool,[26] was found in NC follicles extending from the expected bulge site to dermal cysts (Figure 4 and Figure S6). Noting this result, we further assessed localization of hair follicle differentiation markers, including keratin 6 (K6) (prb-169P, 1:200 dilution; Covance), AE15 (ab58755, 1:100 dilution; Abcam) and AE13 (ab16113, 1:100 dilution; Abcam), which define the companion layer, inner root sheath, and the cuticle and cortex, respectively. K6 was absent within the region of the NC follicular area and cyst (Figure 4). AE13 and AE15 were both absent throughout NC follicles and cysts (Figure 4). Finding an absence of hair follicle differentiation markers in NC, we assessed localization of keratin 10 (K10) (sc-53252, 1:200 dilution; Santa Cruz), a marker of interfollicular epidermal differentiation, which is absent in normal hair follicles. Notably, K10 was ectopically localized suprabasally throughout NC follicles and cysts (Figure 4 and Figure S6). Ki67 (ab15889, 1:300 dilution; Abcam) immunolocalization was performed to assess proliferation, and NC and wild-type skin showed a similar fraction of Ki67-positive basal nuclei, suggesting that comedones are not the direct result of hyperproliferation within follicles or cysts (Figure S7). Presence of the interfollicular epidermis (IFE) marker K10, expansion of the population of cells with K15 immunostaining, and absence of hair-specific markers in NC follicles demonstrates defective differentiation within the NC follicular unit.

Although NEK9 is found in follicle, cyst, and IFE cells, and we have observed via laser capture that somatic mutation is present in both sites (Figure S2), there is no apparent clinical or histologic phenotype in the IFE. Differentiation was assessed via immunolocalization of K10 and filaggrin in the IFE of NC lesional tissue. The localization and immunofluorescence intensity of both markers was identical in normal tissue and in NC IFE (Figure S8).

Mutations in *NEK9* paralogs can cause severe phenotypes. Loss-of-function mutations in *NEK1* cause short-rib polydactyly syndrome (MIM: 263520),[27] and recessive mutations in *NEK8* have been implicated in multiple organ dysplasia (MIM: 615415).[28] Neither NEK1 nor NEK8 have been shown to interact with NEK9 directly.

NEK6, NEK7, and NEK9 are necessary for proper assembly of the mitotic spindle via interaction with EG5, allowing transition from interphase to mitosis.[29] NEK2 separately acts in disassembly of the intercentrosomal linker.[30] Activated NEK9 phosphorylates NEK6 and NEK7,[24,25,31,32] which act on Eg5 to enable chromosome separation and mitotic spindle formation. NEK9 also functions in replication stress response, activating CHK1,[33] and it has been shown to be critical to proliferation in p53-deficient cancer cells, though there is no evidence that NEK9 interacts with p53 directly.[34] Notably, NEK9 has been found to be weakly expressed in normal lung parenchyma, but strongly expressed in lung carcinomas of multiple types, regardless of p53 mutation status, suggesting that it might be important in neoplasia.[34]

Recent reports have shown that recessive germline *NEK9* mutations cause skeletal disease without cutaneous phenotypes. Homozygous nonsense mutations in *NEK9*, c.1489C>T (p.Arg497*), were found in fetuses with a lethal skeletal dysplasia in two Irish Traveller families.[35] In addition, a single affected individual has also been described with a homozygous *NEK9* mutation, demonstrating joint contracture and Legg-Calvé-Perthes (MIM: 150600) disease.[36] Notably, NC syndrome features skeletal abnormalities, including scoliosis, syndactyly or absence of fingers, and supranumerary digits, suggesting that somatic *NEK9* mutation in bone progenitors could account for these findings.[37]

Overexpression or knockout of NEK9 and its effectors leads to severe cellular dysfunction. NEK9 silencing via RNAi in cell culture prevents effective mitosis, leading to weak or malformed mitotic spindles.[25] Further, overexpression of NEK9 in cells is toxic, with the majority of transiently transfected cells unable to successfully progress through a mitotic cycle.[24] Similarly severe findings are found with lesions in downstream effectors of NEK9 signaling. Mice with deletion of NEK7 have early mortality due to failure in cytokinesis, and embryonic fibroblasts from NEK7-null animals were found to be polyploid with abnormal cilia morphology.[38] Mice overexpressing Eg5 demonstrate increased propensity for tumors and genomic instability with poor chromosome segregation.[39]

Despite a known role in spindle formation and chromosome separation and in checkpoint regulation, our results further suggest that NEK9 might have additional function in the epidermis. In NC lesional tissue, the ectopic strong basal layer localization of K15 in comedonal follicles and cysts and simultaneous suprabasal localization of K10 suggests a switch in fate of progenitors from hair follicle to an IFE-like lineage. This switch might account for differentiation defects in NC, which bear some similarities to those seen in mouse models featuring cystic hair follicles and IFE-specific localization of differentiation markers in follicular keratinocytes.[40–42]

Mice with decreased LEF1 signaling due to deletion of the beta-catenin binding domain of LEF1 develop dermal cysts that resemble those found in NC on histopathologic examination. As in NC, these cysts demonstrate suprabasal K10, but immunolocalization of keratin 6 (K6) is present in cysts and hair follicles, a finding not seen in NC cysts or follicles.[42] Similarly, defects in Notch signaling due to loss of mesenchymal RBP-Jκ can lead to K10-positive cyst formation. These lose AE13 and AE15 as seen in NC but retain K6.[40] Finally, K15 conditional *SOX9* knockout mice also develop K10-positive cysts in hair follicles, though these show normal K6, AE13, and AE15 immunolocalization, unlike NC.[41]

These mouse models demonstrate that several pathways, involving both epidermal and mesenchymal inputs, can alter hair follicle progenitor fate. In NC, the loss of normal follicular differentiation markers, expansion of strongly K15-positive basal cells, and suprabasal localization of K10 throughout the follicle and cyst suggests that NC demonstrates a similar type of fate switching. This "fate switch" paradigm might partly help explain why NC has no evident IFE pathology; if *NEK9* mutation drives cells toward an IFE fate, one might expect that cells intended for such a fate would be less affected or unaffected.

The discovery of somatic *NEK9* mutations at highly conserved sites in three unrelated NC cases, with no evidence for additional somatic mutations within the lesions, demonstrates that somatic *NEK9* mutation causes NC. *NEK9* mutations in NC resulted in increased Thr210 phosphorylation, suggesting gain of function, and affected tissue showed loss of markers of follicular differentiation with concurrent gain of an IFE marker. Although NEK9 localizes to cells within the IFE and hair follicle (Figure S5), is highly conserved across species (Figure S4), and is known to act in pathways regulating cell-cycle and checkpoint control,[29] our results suggest that NEK9 might also co-regulate pathways relevant to follicular cell fate. Given the aforementioned mouse models featuring phenotypes similar to NC, it is plausible that NEK9 might function in the Wnt, Notch, or Sox9 signaling pathways. Future experiments addressing these possibilities could reveal a role for NEK9 in hair follicle fate decisions.

Given that comedone formation is critical step in acne pathogenesis and that *NEK9* mutations in NC appear to have a follicle-specific effect, it is intriguing to consider

whether NEK9 and its effectors might contribute to acne vulgaris pathobiology.

Accession Numbers

The accession number for the sequencing data reported in this paper is dbGAP: phs000744.

Supplemental Data

Supplemental Data include eight figures and two tables and can be found with this article online at http://dx.doi.org/10.1016/j.ajhg.2016.03.019.

Acknowledgments

We would like to thank Valerie Horsley, Richard Lifton, Young Lim, Haris Mirza, Lynn Boyden, and Peggy Myung for review of the manuscript. We would also like to thank Jing Zhou and Rong Hua Hu for technical assistance. Research was supported by the Doris Duke Charitable Foundation Clinical Scientist Development Award to K.A.C. and a Yale Center for Mendelian Genomics grant (NIH U54 HG006504). J.L.L. is supported by the Medical Scientist Training Program (NIH NIGMS GM007205) at Yale University and is a recipient of a clinical research mentorship award from the Doris Duke Charitable Foundation. J.L.S. is an investigator for Galderma, Ranbaxy, and Activis, a consultant for Galderma, and a Medical Safety Monitor for Seegpharm and Valeant.

Received: January 6, 2016
Accepted: March 16, 2016
Published: May 5, 2016

Web Resources

1000 Genomes, http://www.1000genomes.org
dbSNP, http://www.ncbi.nlm.nih.gov/projects/SNP/
dbGaP, http://www.ncbi.nlm.nih.gov/gap
ExAC Browser, http://exac.broadinstitute.org/
GATK, https://www.broadinstitute.org/gatk/
GenBank, http://www.ncbi.nlm.nih.gov/genbank/
MuTect, https://www.broadinstitute.org/cancer/cga/mutect
NHLBI Exome Sequencing Project (ESP) Exome Variant Server, http://evs.gs.washington.edu/EVS/
OMIM, http://www.omim.org/
UCSC Genome Browser, http://genome.ucsc.edu

References

1. Cunliffe, W.J., Holland, D.B., and Jeremy, A. (2004). Comedone formation: etiology, clinical presentation, and treatment. Clin. Dermatol. *22*, 367–374.
2. Williams, H.C., Dellavalle, R.P., and Garner, S. (2012). Acne vulgaris. Lancet *379*, 361–372.
3. Toyoda, M., and Morohashi, M. (2001). Pathogenesis of acne. Med. Electron Microsc. *34*, 29–40.
4. Zouboulis, C.C., and Bettoli, V. (2015). Management of severe acne. Br. J. Dermatol. *172* (*Suppl 1*), 27–36.
5. Wilkie, A.O., Slaney, S.F., Oldridge, M., Poole, M.D., Ashworth, G.J., Hockley, A.D., Hayward, R.D., David, D.J., Pulleyn, L.J., Rutland, P., et al. (1995). Apert syndrome results from localized mutations of FGFR2 and is allelic with Crouzon syndrome. Nat. Genet. *9*, 165–172.
6. Munro, C.S., and Wilkie, A.O. (1998). Epidermal mosaicism producing localised acne: somatic mutation in FGFR2. Lancet *352*, 704–705.
7. Grose, R., Fantl, V., Werner, S., Chioni, A.M., Jarosz, M., Rudling, R., Cross, B., Hart, I.R., and Dickson, C. (2007). The role of fibroblast growth factor receptor 2b in skin homeostasis and cancer development. EMBO J. *26*, 1268–1278.
8. Petiot, A., Conti, F.J., Grose, R., Revest, J.M., Hodivala-Dilke, K.M., and Dickson, C. (2003). A crucial role for Fgfr2-IIIb signalling in epidermal development and hair follicle patterning. Development *130*, 5493–5501.
9. Jansen, T., and Plewig, G. (1998). Acne inversa. Int. J. Dermatol. *37*, 96–100.
10. Wang, B., Yang, W., Wen, W., Sun, J., Su, B., Liu, B., Ma, D., Lv, D., Wen, Y., Qu, T., et al. (2010). Gamma-secretase gene mutations in familial acne inversa. Science *330*, 1065.
11. Pink, A.E., Simpson, M.A., Desai, N., Trembath, R.C., and Barker, J.N. (2013). γ-Secretase mutations in hidradenitis suppurativa: new insights into disease pathogenesis. J. Invest. Dermatol. *133*, 601–607.
12. He, L., Wu, W.J., Yang, J.K., Cheng, H., Zuo, X.B., Lai, W., Gao, T.W., Ma, C.L., Luo, N., Huang, J.Q., et al. (2014). Two new susceptibility loci 1q24.2 and 11p11.2 confer risk to severe acne. Nat. Commun. *5*, 2870.
13. Navarini, A.A., Simpson, M.A., Weale, M., Knight, J., Carlavan, I., Reiniche, P., Burden, D.A., Layton, A., Bataille, V., Allen, M., et al.; Acne Genetic Study Group (2014). Genome-wide association study identifies three novel susceptibility loci for severe Acne vulgaris. Nat. Commun. *5*, 4020.
14. Zhang, M., Qureshi, A.A., Hunter, D.J., and Han, J. (2014). A genome-wide association study of severe teenage acne in European Americans. Hum. Genet. *133*, 259–264.
15. Tchernev, G., Ananiev, J., Semkova, K., Dourmishev, L.A., Schönlebe, J., and Wollina, U. (2013). Nevus comedonicus: an updated review. Dermatol. Ther. (Heidelb.) *3*, 33–40.
16. Moss, C., Larkins, S., Stacey, M., Blight, A., Farndon, P.A., and Davison, E.V. (1993). Epidermal mosaicism and Blaschko's lines. J. Med. Genet. *30*, 752–755.
17. Lim, Y.H., Ovejero, D., Sugarman, J.S., Deklotz, C.M., Maruri, A., Eichenfield, L.F., Kelley, P.K., Jüppner, H., Gottschalk, M., Tifft, C.J., et al. (2014). Multilineage somatic activating mutations in HRAS and NRAS cause mosaic cutaneous and skeletal lesions, elevated FGF23 and hypophosphatemia. Hum. Mol. Genet. *23*, 397–407.
18. Happle, R. (2010). The group of epidermal nevus syndromes Part I. Well defined phenotypes. J. Am. Acad. Dermatol. *63*, 1–22.
19. Solomon, L.M., Fretzin, D., and Pruzansky, S. (1970). Pilosebaceous abnormalities in Apert's syndrome. Arch. Dermatol. *102*, 381–385.
20. Li, H., and Durbin, R. (2009). Fast and accurate short read alignment with Burrows-Wheeler transform. Bioinformatics *25*, 1754–1760.
21. Van der Auwera, G.A., Carneiro, M.O., Hartl, C., Poplin, R., Del Angel, G., Levy-Moonshine, A., Jordan, T., Shakir, K., Roazen, D., Thibault, J., et al. (2013). From FastQ data to high confidence variant calls: the Genome Analysis Toolkit best practices pipeline. Curr Protoc Bioinformatics, 11, 11 10 11-11 10 33.

22. Cibulskis, K., Lawrence, M.S., Carter, S.L., Sivachenko, A., Jaffe, D., Sougnez, C., Gabriel, S., Meyerson, M., Lander, E.S., and Getz, G. (2013). Sensitive detection of somatic point mutations in impure and heterogeneous cancer samples. Nat. Biotechnol. *31*, 213–219.
23. Wang, K., Li, M., and Hakonarson, H. (2010). ANNOVAR: functional annotation of genetic variants from high-throughput sequencing data. Nucleic Acids Res. *38*, e164.
24. Roig, J., Mikhailov, A., Belham, C., and Avruch, J. (2002). Nercc1, a mammalian NIMA-family kinase, binds the Ran GTPase and regulates mitotic progression. Genes Dev. *16*, 1640–1658.
25. Bertran, M.T., Sdelci, S., Regué, L., Avruch, J., Caelles, C., and Roig, J. (2011). Nek9 is a Plk1-activated kinase that controls early centrosome separation through Nek6/7 and Eg5. EMBO J. *30*, 2634–2647.
26. Bose, A., Teh, M.T., Mackenzie, I.C., and Waseem, A. (2013). Keratin k15 as a biomarker of epidermal stem cells. Int. J. Mol. Sci. *14*, 19385–19398.
27. Thiel, C., Kessler, K., Giessl, A., Dimmler, A., Shalev, S.A., von der Haar, S., Zenker, M., Zahnleiter, D., Stöss, H., Beinder, E., et al. (2011). NEK1 mutations cause short-rib polydactyly syndrome type majewski. Am. J. Hum. Genet. *88*, 106–114.
28. Frank, V., Habbig, S., Bartram, M.P., Eisenberger, T., Veenstra-Knol, H.E., Decker, C., Boorsma, R.A., Göbel, H., Nürnberg, G., Griessmann, A., et al. (2013). Mutations in NEK8 link multiple organ dysplasia with altered Hippo signalling and increased c-MYC expression. Hum. Mol. Genet. *22*, 2177–2185.
29. Sdelci, S., Bertran, M.T., and Roig, J. (2011). Nek9, Nek6, Nek7 and the separation of centrosomes. Cell Cycle *10*, 3816–3817.
30. Bahmanyar, S., Kaplan, D.D., Deluca, J.G., Giddings, T.H., Jr., O'Toole, E.T., Winey, M., Salmon, E.D., Casey, P.J., Nelson, W.J., and Barth, A.I. (2008). beta-Catenin is a Nek2 substrate involved in centrosome separation. Genes Dev. *22*, 91–105.
31. Roig, J., Groen, A., Caldwell, J., and Avruch, J. (2005). Active Nercc1 protein kinase concentrates at centrosomes early in mitosis and is necessary for proper spindle assembly. Mol. Biol. Cell *16*, 4827–4840.
32. Belham, C., Roig, J., Caldwell, J.A., Aoyama, Y., Kemp, B.E., Comb, M., and Avruch, J. (2003). A mitotic cascade of NIMA family kinases. Nercc1/Nek9 activates the Nek6 and Nek7 kinases. J. Biol. Chem. *278*, 34897–34909.
33. Smith, S.C., Petrova, A.V., Madden, M.Z., Wang, H., Pan, Y., Warren, M.D., Hardy, C.W., Liang, D., Liu, E.A., Robinson, M.H., et al. (2014). A gemcitabine sensitivity screen identifies a role for NEK9 in the replication stress response. Nucleic Acids Res. *42*, 11517–11527.
34. Kurioka, D., Takeshita, F., Tsuta, K., Sakamoto, H., Watanabe, S., Matsumoto, K., Watanabe, M., Nakagama, H., Ochiya, T., Yokota, J., et al. (2014). NEK9-dependent proliferation of cancer cells lacking functional p53. Sci. Rep. *4*, 6111.
35. Casey, J.P., Brennan, K., Scheidel, N., McGettigan, P., Lavin, P.T., Carter, S., Ennis, S., Dorkins, H., Ghali, N., Blacque, O.E., et al. (2016). Recessive NEK9 mutation causes a lethal skeletal dysplasia with evidence of cell cycle and ciliary defects. Hum. Mol. Genet. Published online February 21, 2016. http://dx.doi.org/10.1093/hmg/ddw054.
36. Shaheen, R., Patel, N., Shamseldin, H., Alzahrani, F., Al-Yamany, R., ALMoisheer, A., Ewida, N., Anazi, S., Alnemer, M., Elsheikh, M., et al. (2015). Accelerating matchmaking of novel dysmorphology syndromes through clinical and genomic characterization of a large cohort. Genet. Med. Published online December 3, 2015. http://dx.doi.org/10.1038/gim.2015.147.
37. Beck, M.H., and Dave, V.K. (1980). Extensive nevus comedonicus. Arch. Dermatol. *116*, 1048–1050.
38. Salem, H., Rachmin, I., Yissachar, N., Cohen, S., Amiel, A., Haffner, R., Lavi, L., and Motro, B. (2010). Nek7 kinase targeting leads to early mortality, cytokinesis disturbance and polyploidy. Oncogene *29*, 4046–4057.
39. Castillo, A., Morse, H.C., 3rd, Godfrey, V.L., Naeem, R., and Justice, M.J. (2007). Overexpression of Eg5 causes genomic instability and tumor formation in mice. Cancer Res. *67*, 10138–10147.
40. Hu, B., Lefort, K., Qiu, W., Nguyen, B.C., Rajaram, R.D., Castillo, E., He, F., Chen, Y., Angel, P., Brisken, C., and Dotto, G.P. (2010). Control of hair follicle cell fate by underlying mesenchyme through a CSL-Wnt5a-FoxN1 regulatory axis. Genes Dev. *24*, 1519–1532.
41. Kadaja, M., Keyes, B.E., Lin, M., Pasolli, H.A., Genander, M., Polak, L., Stokes, N., Zheng, D., and Fuchs, E. (2014). SOX9: a stem cell transcriptional regulator of secreted niche signaling factors. Genes Dev. *28*, 328–341.
42. Niemann, C., Owens, D.M., Hülsken, J., Birchmeier, W., and Watt, F.M. (2002). Expression of DeltaNLef1 in mouse epidermis results in differentiation of hair follicles into squamous epidermal cysts and formation of skin tumours. Development *129*, 95–109.

The American Journal of Human Genetics, Volume *98*

Supplemental Data

Somatic Mutations in *NEK9* Cause Nevus Comedonicus

Jonathan L. Levinsohn, Jeffrey L. Sugarman, Yale Center for Mendelian Genomics, Jennifer M. McNiff, Richard J. Antaya, and Keith A. Choate

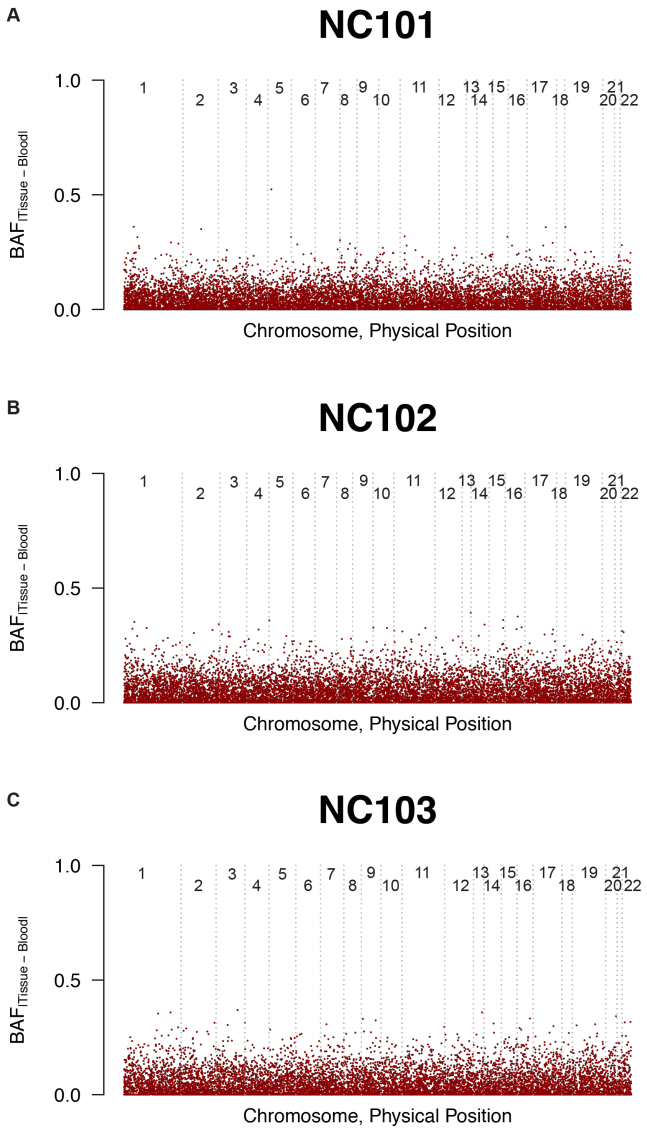

Supplemental Figure 1. NC lesions demonstrate no regions of loss of heterozygosity. Difference of B-allele frequency between tissue and blood is plotted against genomic position, demonstrating no regions with altered B-allele frequency. There is no evidence of large segments of loss of heterozygosity in any of the samples.

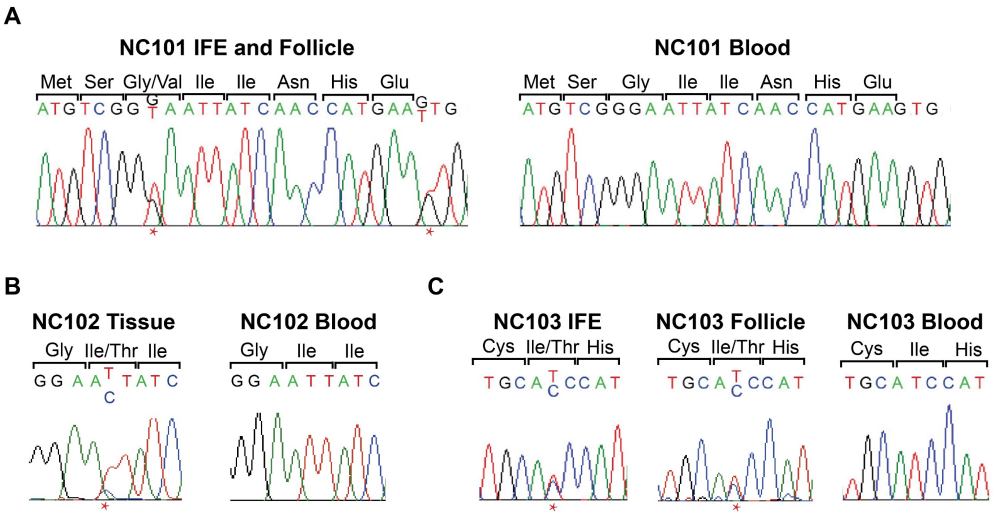

Supplemental Figure 2. Sanger sequencing confirms somatic mutations identified via whole exome sequencing. Sanger sequencing of PCR amplified gDNA isolated from laser-captured IFE and follicle tissue for NC101 (A) confirms two mutations. One mutation is at p.Gly572Val, creating a cryptic splice donor site, and the other mutation destroys the normal splice donor site, leading to deletion of Gly572 through Glu577 (Figure S3). These mutations are absent in blood. Sanger sequencing of NC102 gDNA also confirms the p.Ile573Thr mutation is present in DNA isolated from whole affected tissue (B), but is absent in blood. Sanger sequence of laser-captured IFE and follicle tissue NC103 (C) confirms a somatic p.Ile167Thr mutation in IFE and in follicle.

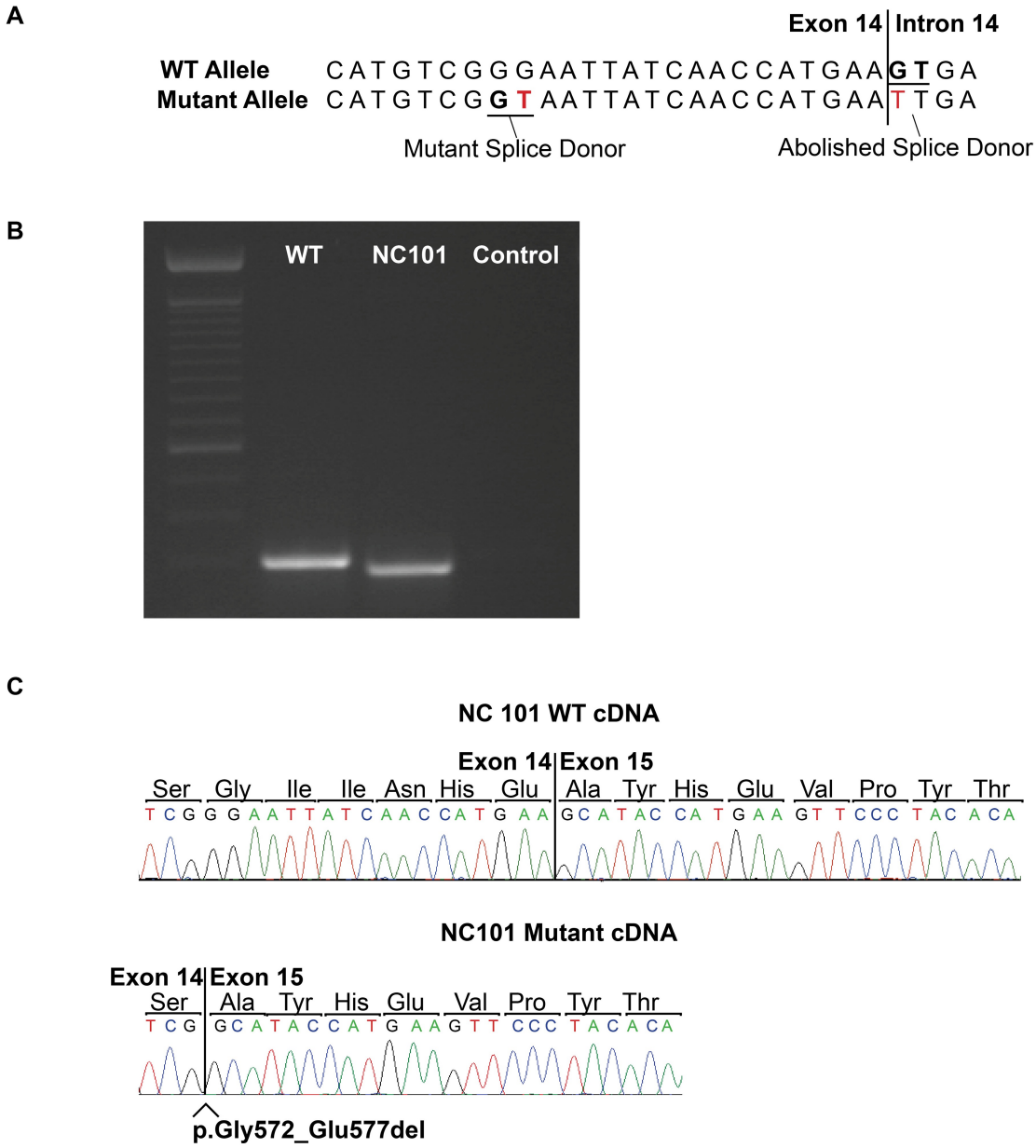

Supplemental Figure 3. Analysis of *NEK9* splicing mutation in NC101 tissue reveals a 6 amino acid deletion. Two mutations are present in NC101 tissue in *cis*. The first mutation appears to abolish a splice donor, and the second mutation creates a potential novel upstream splice donor (A). To experimentally assess the consequence of this mutant allele upon encoded RNA, high-fidelity Advantage II long range PCR (Clontech) of genomic DNA from NC101 was used to create amplicons consisting of exons 13-15 including flanking intronic regions. This amplicon was TA-cloned (Invitrogen). Clones were sequenced to confirm that they contained the mutant allele without additional mutations introduced by PCR, and were then cloned into pCDNA 3.1 using Kpn1 and Not1. WT and mutant plasmids were transfected into PLC cells. 48 hours after transfection, RNA was

isolated using the RNEasy kit (QIAGEN). cDNA was generated using the iScript kit (BD Biosciences). PCR was then performed and products were run on a 1% agarose gel (B) demonstrating that NC101 mutant allele cDNA was shorter than the WT allele. Sanger sequencing of these products revealed that the NC101 mutant lacked 18 nucleotides encoding amino acids ‘Gly,Ile,Ile,Asn,His,Glu’ which fall within the RCC1 domain (C).

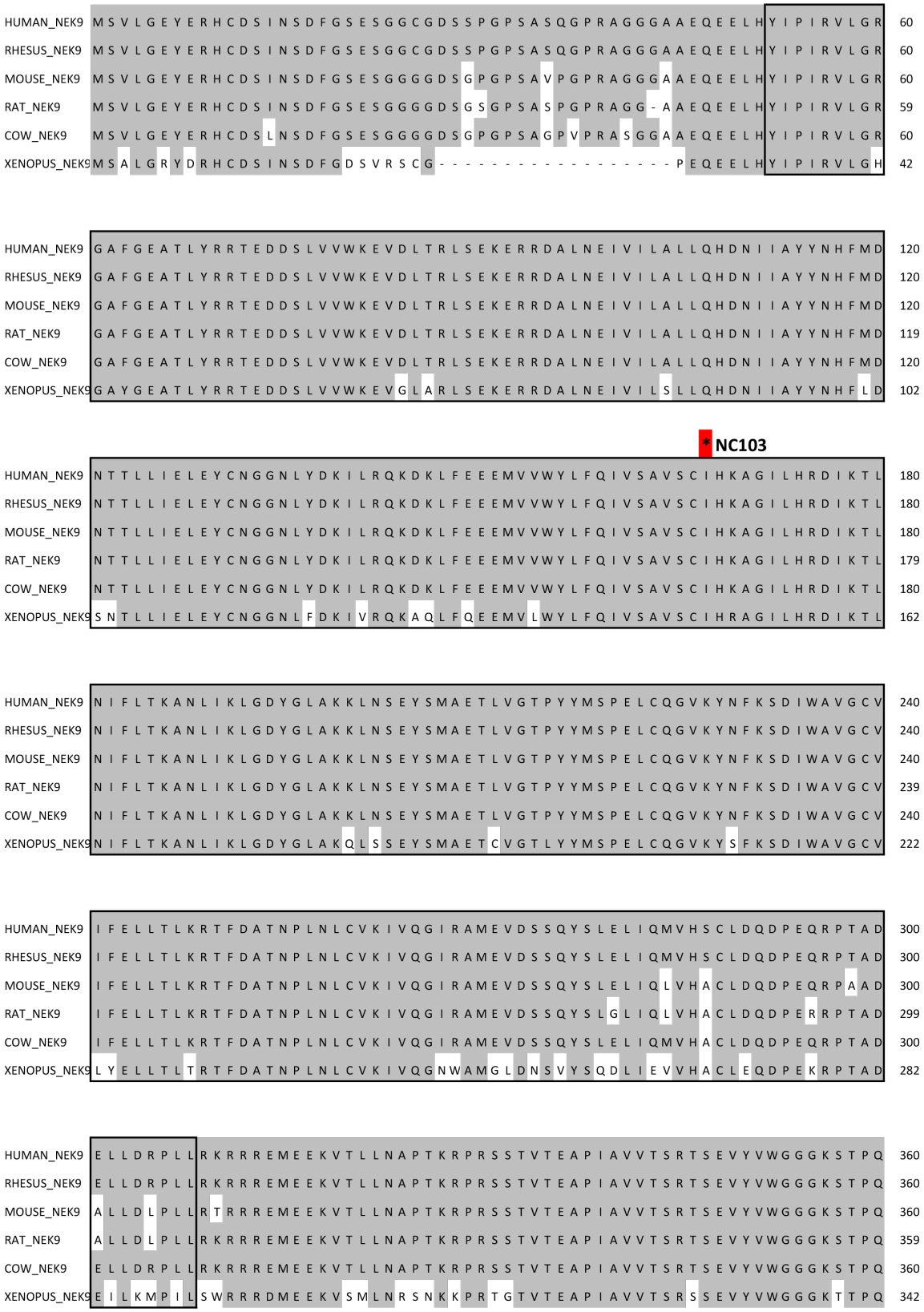
HUMAN_NEK9 MSVLGEYERHCDSINSDFGSESGGCGDSSPGPSASQGPRAGGGAAEQEELHYIPIRVLGR 60
RHESUS_NEK9 MSVLGEYERHCDSINSDFGSESGGCGDSSPGPSASQGPRAGGGAAEQEELHYIPIRVLGR 60
MOUSE_NEK9 MSVLGEYERHCDSINSDFGSESGGGGDSGPGPSAVPGPRAGGGAAEQEELHYIPIRVLGR 60
RAT_NEK9 MSVLGEYERHCDSINSDFGSESGGGGDSGSGPSASPGPRAGG-AAEQEELHYIPIRVLGR 59
COW_NEK9 MSVLGEYERHCDSLNSDFGSESGGGGDSGPGPSAGPVPRASGGAAEQEELHYIPIRVLGR 60
XENOPUS_NEK9 MSALGRYDRHCDSINSDFGDSVRSCG----------PEQEELHYIPIRVLGH 42
HUMAN_NEK9 GAFGEATLYRRTEDDSLVVWKEVDLTRLSEKERRDALNEIVILALLQHDNIIAYYNHFMD 120
RHESUS_NEK9 GAFGEATLYRRTEDDSLVVWKEVDLTRLSEKERRDALNEIVILALLQHDNIIAYYNHFMD 120
MOUSE_NEK9 GAFGEATLYRRTEDDSLVVWKEVDLTRLSEKERRDALNEIVILALLQHDNIIAYYNHFMD 120
RAT_NEK9 GAFGEATLYRRTEDDSLVVWKEVDLTRLSEKERRDALNEIVILALLQHDNIIAYYNHFMD 119
COW_NEK9 GAFGEATLYRRTEDDSLVVWKEVDLTRLSEKERRDALNEIVILALLQHDNIIAYYNHFMD 120
XENOPUS_NEK9 GAYGEATLYRRTEDDSLVVWKEVGLARLSEKERRDALNEIVILSLLQHDNIIAYYNHFLD 102
*NC103
HUMAN_NEK9 NTTLLIELEYCNGGNLYDKILRQKDKLFEEEMVVWYLFQIVSAVSCIHKAGILHRDIKTL 180
RHESUS_NEK9 NTTLLIELEYCNGGNLYDKILRQKDKLFEEEMVVWYLFQIVSAVSCIHKAGILHRDIKTL 180
MOUSE_NEK9 NTTLLIELEYCNGGNLYDKILRQKDKLFEEEMVVWYLFQIVSAVSCIHKAGILHRDIKTL 180
RAT_NEK9 NTTLLIELEYCNGGNLYDKILRQKDKLFEEEMVVWYLFQIVSAVSCIHKAGILHRDIKTL 179
COW_NEK9 NTTLLIELEYCNGGNLYDKILRQKDKLFEEEMVVWYLFQIVSAVSCIHKAGILHRDIKTL 180
XENOPUS_NEK9 SNTLLIELEYCNGGNLFDKIVRQKAQLFQEEMVLWYLFQIVSAVSCIHRAGILHRDIKTL 162
HUMAN_NEK9 NIFLTKANLIKLGDYGLAKKLNSEYSMAETLVGTPYYMSPELCQGVKYNFKSDIWAVGCV 240
RHESUS_NEK9 NIFLTKANLIKLGDYGLAKKLNSEYSMAETLVGTPYYMSPELCQGVKYNFKSDIWAVGCV 240
MOUSE_NEK9 NIFLTKANLIKLGDYGLAKKLNSEYSMAETLVGTPYYMSPELCQGVKYNFKSDIWAVGCV 240
RAT_NEK9 NIFLTKANLIKLGDYGLAKKLNSEYSMAETLVGTPYYMSPELCQGVKYNFKSDIWAVGCV 239
COW_NEK9 NIFLTKANLIKLGDYGLAKKLNSEYSMAETLVGTPYYMSPELCQGVKYNFKSDIWAVGCV 240
XENOPUS_NEK9 NIFLTKANLIKLGDYGLAKQLSSEYSMAETCVGTLYYMSPELCQGVKYSFKSDIWAVGCV 222
HUMAN_NEK9 IFELLTLKRTFDATNPLNLCVKIVQGIRAMEVDSSQYSLELIQMVHSCLDQDPEQRPTAD 300
RHESUS_NEK9 IFELLTLKRTFDATNPLNLCVKIVQGIRAMEVDSSQYSLELIQMVHSCLDQDPEQRPTAD 300
MOUSE_NEK9 IFELLTLKRTFDATNPLNLCVKIVQGIRAMEVDSSQYSLELIQLVHACLDQDPEQRPAAD 300
RAT_NEK9 IFELLTLKRTFDATNPLNLCVKIVQGIRAMEVDSSQYSLGLIQLVHACLDQDPERRPTAD 299
COW_NEK9 IFELLTLKRTFDATNPLNLCVKIVQGIRAMEVDSSQYSLELIQMVHACLDQDPEQRPTAD 300
XENOPUS_NEK9 LYELLTLTRTFDATNPLNLCVKIVQGNWAMGLDNSVYSQDLIEVVHACLEQDPEKRPTAD 282
HUMAN_NEK9 ELLDRPLLRKRRREMEEKVTLLNAPTKRPRSSTVTEAPIAVVTSRTSEVYVWGGGKSTPQ 360
RHESUS_NEK9 ELLDRPLLRKRRREMEEKVTLLNAPTKRPRSSTVTEAPIAVVTSRTSEVYVWGGGKSTPQ 360
MOUSE_NEK9 ALLDLPLLRTRRREMEEKVTLLNAPTKRPRSSTVTEAPIAVVTSRTSEVYVWGGGKSTPQ 360
RAT_NEK9 ALLDLPLLRKRRREMEEKVTLLNAPTKRPRSSTVTEAPIAVVTSRTSEVYVWGGGKSTPQ 359
COW_NEK9 ELLDRPLLRKRRREMEEKVTLLNAPTKRPRSSTVTEAPIAVVTSRTSEVYVWGGGKSTPQ 360
XENOPUS_NEK9 EILKMPILSWRRRDMEEKVSMLNRSNKKPRTGTVTEAPIAVVTSRSSEVYVWGGGKTTPQ 342

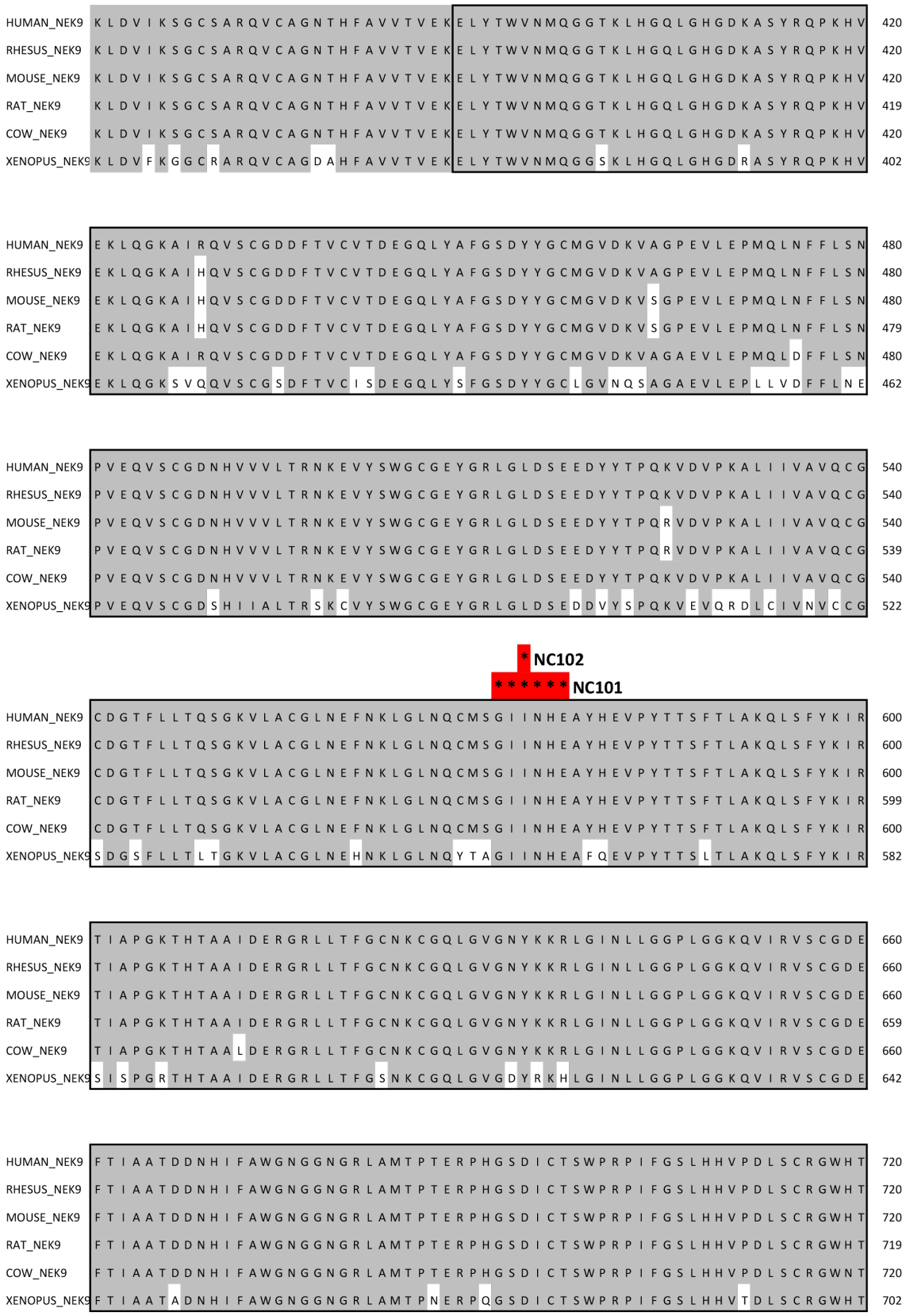
HUMAN_NEK9 K L D V I K S G C S A R Q V C A G N T H F A V V T V E K E L Y T W V N M Q G G T K L H G Q L G H G D K A S Y R Q P K H V 420
RHESUS_NEK9 K L D V I K S G C S A R Q V C A G N T H F A V V T V E K E L Y T W V N M Q G G T K L H G Q L G H G D K A S Y R Q P K H V 420
MOUSE_NEK9 K L D V I K S G C S A R Q V C A G N T H F A V V T V E K E L Y T W V N M Q G G T K L H G Q L G H G D K A S Y R Q P K H V 420
RAT_NEK9 K L D V I K S G C S A R Q V C A G N T H F A V V T V E K E L Y T W V N M Q G G T K L H G Q L G H G D K A S Y R Q P K H V 419
COW_NEK9 K L D V I K S G C S A R Q V C A G N T H F A V V T V E K E L Y T W V N M Q G G T K L H G Q L G H G D K A S Y R Q P K H V 420
XENOPUS_NEK9 K L D V F K G G C R A R Q V C A G D A H F A V V T V E K E L Y T W V N M Q G G S K L H G Q L G H G D R A S Y R Q P K H V 402
HUMAN_NEK9 E K L Q G K A I R Q V S C G D D F T V C V T D E G Q L Y A F G S D Y Y G C M G V D K V A G P E V L E P M Q L N F F L S N 480
RHESUS_NEK9 E K L Q G K A I H Q V S C G D D F T V C V T D E G Q L Y A F G S D Y Y G C M G V D K V A G P E V L E P M Q L N F F L S N 480
MOUSE_NEK9 E K L Q G K A I H Q V S C G D D F T V C V T D E G Q L Y A F G S D Y Y G C M G V D K V S G P E V L E P M Q L N F F L S N 480
RAT_NEK9 E K L Q G K A I H Q V S C G D D F T V C V T D E G Q L Y A F G S D Y Y G C M G V D K V S G P E V L E P M Q L N F F L S N 479
COW_NEK9 E K L Q G K A I R Q V S C G D D F T V C V T D E G Q L Y A F G S D Y Y G C M G V D K V A G A E V L E P M Q L D F F L S N 480
XENOPUS_NEK9 E K L Q G K S V Q Q V S C G S D F T V C I S D E G Q L Y S F G S D Y Y G C L G V N Q S A G A E V L E P L L V D F F L N E 462
HUMAN_NEK9 P V E Q V S C G D N H V V V L T R N K E V Y S W G C G E Y G R L G L D S E E D Y Y T P Q K V D V P K A L I I V A V Q C G 540
RHESUS_NEK9 P V E Q V S C G D N H V V V L T R N K E V Y S W G C G E Y G R L G L D S E E D Y Y T P Q K V D V P K A L I I V A V Q C G 540
MOUSE_NEK9 P V E Q V S C G D N H V V V L T R N K E V Y S W G C G E Y G R L G L D S E E D Y Y T P Q R V D V P K A L I I V A V Q C G 540
RAT_NEK9 P V E Q V S C G D N H V V V L T R N K E V Y S W G C G E Y G R L G L D S E E D Y Y T P Q R V D V P K A L I I V A V Q C G 539
COW_NEK9 P V E Q V S C G D N H V V V L T R N K E V Y S W G C G E Y G R L G L D S E E D Y Y T P Q K V D V P K A L I I V A V Q C G 540
XENOPUS_NEK9 P V E Q V S C G D S H I I A L T R S K C V Y S W G C G E Y G R L G L D S E D D V Y S P Q K V E V Q R D L C I V N V C C G 522
* NC102
***** NC101
HUMAN_NEK9 C D G T F L L T Q S G K V L A C G L N E F N K L G L N Q C M S G I I N H E A Y H E V P Y T T S F T L A K Q L S F Y K I R 600
RHESUS_NEK9 C D G T F L L T Q S G K V L A C G L N E F N K L G L N Q C M S G I I N H E A Y H E V P Y T T S F T L A K Q L S F Y K I R 600
MOUSE_NEK9 C D G T F L L T Q S G K V L A C G L N E F N K L G L N Q C M S G I I N H E A Y H E V P Y T T S F T L A K Q L S F Y K I R 600
RAT_NEK9 C D G T F L L T Q S G K V L A C G L N E F N K L G L N Q C M S G I I N H E A Y H E V P Y T T S F T L A K Q L S F Y K I R 599
COW_NEK9 C D G T F L L T Q S G K V L A C G L N E F N K L G L N Q C M S G I I N H E A Y H E V P Y T T S F T L A K Q L S F Y K I R 600
XENOPUS_NEK9 S D G S F L L T L T G K V L A C G L N E H N K L G L N Q Y T A G I I N H E A F Q E V P Y T T S L T L A K Q L S F Y K I R 582
HUMAN_NEK9 T I A P G K T H T A A I D E R G R L L T F G C N K C G Q L G V G N Y K K R L G I N L L G G P L G G K Q V I R V S C G D E 660
RHESUS_NEK9 T I A P G K T H T A A I D E R G R L L T F G C N K C G Q L G V G N Y K K R L G I N L L G G P L G G K Q V I R V S C G D E 660
MOUSE_NEK9 T I A P G K T H T A A I D E R G R L L T F G C N K C G Q L G V G N Y K K R L G I N L L G G P L G G K Q V I R V S C G D E 660
RAT_NEK9 T I A P G K T H T A A I D E R G R L L T F G C N K C G Q L G V G N Y K K R L G I N L L G G P L G G K Q V I R V S C G D E 659
COW_NEK9 T I A P G K T H T A A L D E R G R L L T F G C N K C G Q L G V G N Y K K R L G I N L L G G P L G G K Q V I R V S C G D E 660
XENOPUS_NEK9 S I S P G R T H T A A I D E R G R L L T F G S N K C G Q L G V G D Y R K H L G I N L L G G P L G G K Q V I R V S C G D E 642
HUMAN_NEK9 F T I A A T D D N H I F A W G N G G N G R L A M T P T E R P H G S D I C T S W P R P I F G S L H H V P D L S C R G W H T 720
RHESUS_NEK9 F T I A A T D D N H I F A W G N G G N G R L A M T P T E R P H G S D I C T S W P R P I F G S L H H V P D L S C R G W H T 720
MOUSE_NEK9 F T I A A T D D N H I F A W G N G G N G R L A M T P T E R P H G S D I C T S W P R P I F G S L H H V P D L S C R G W H T 720
RAT_NEK9 F T I A A T D D N H I F A W G N G G N G R L A M T P T E R P H G S D I C T S W P R P I F G S L H H V P D L S C R G W H T 719
COW_NEK9 F T I A A T D D N H I F A W G N G G N G R L A M T P T E R P H G S D I C T S W P R P I F G S L H H V P D L S C R G W N T 720
XENOPUS_NEK9 F T I A A T A D N H I F A W G N G G N G R L A M T P N E R P Q G S D I C T S W P R P I F G S L H H V T D L S C R G W H T 702

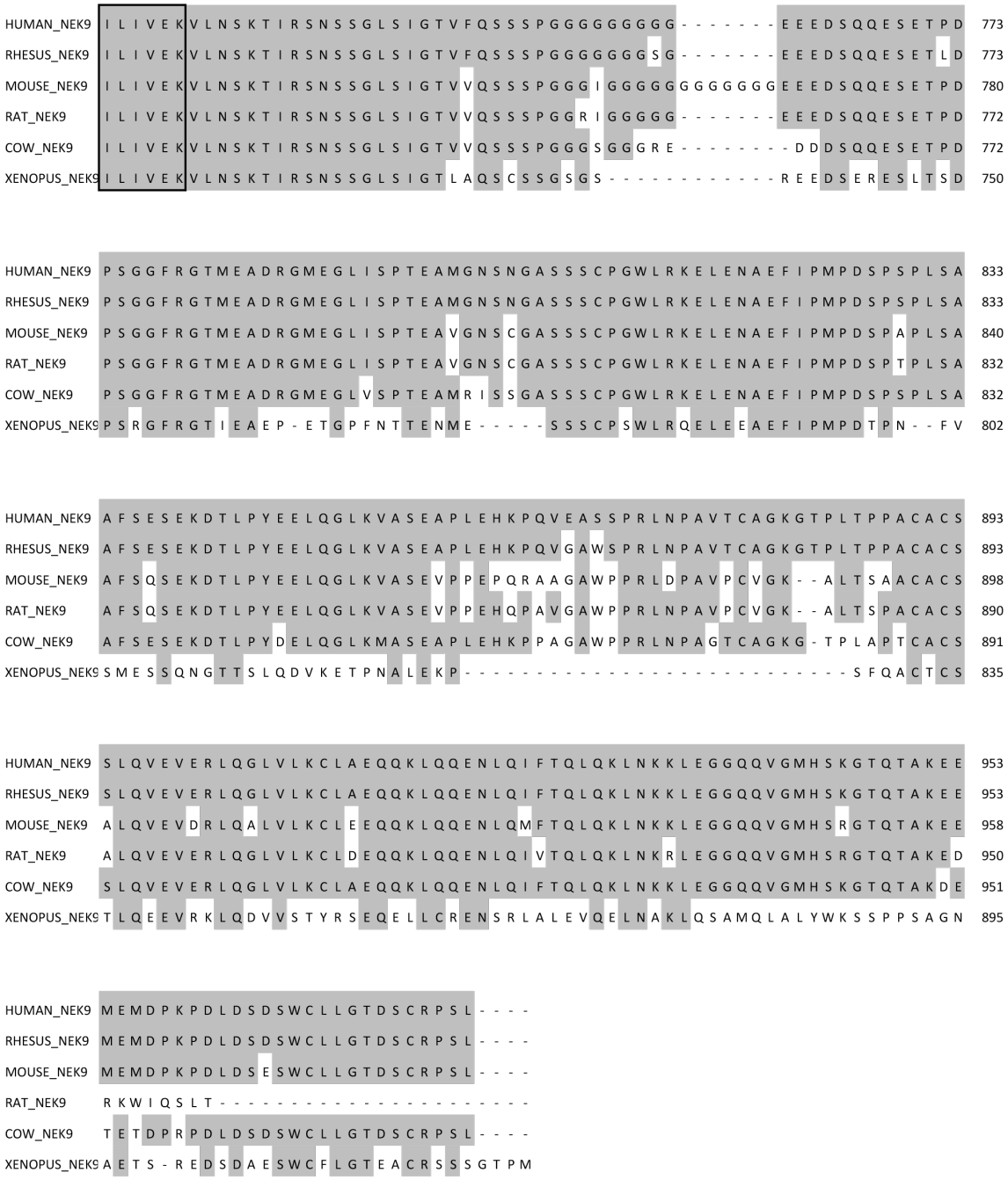

Supplemental Figure 4. NC101, NC102 and NC103 mutations are at conserved residues. Human, rhesus, mouse, rat, cow and *Xenopus NEK9* orthologs were aligned using CLUSTAL-omega. The amino acids affected by NC101, NC102 and NC103 mutations are indicated by a red asterisk above the amino acid(s) involved. All mutations affect amino acids that are highly conserved across vertebrate species. The kinase domain (residues 52-308) and RCC1 domain (residues 388-726) are outlined in black.

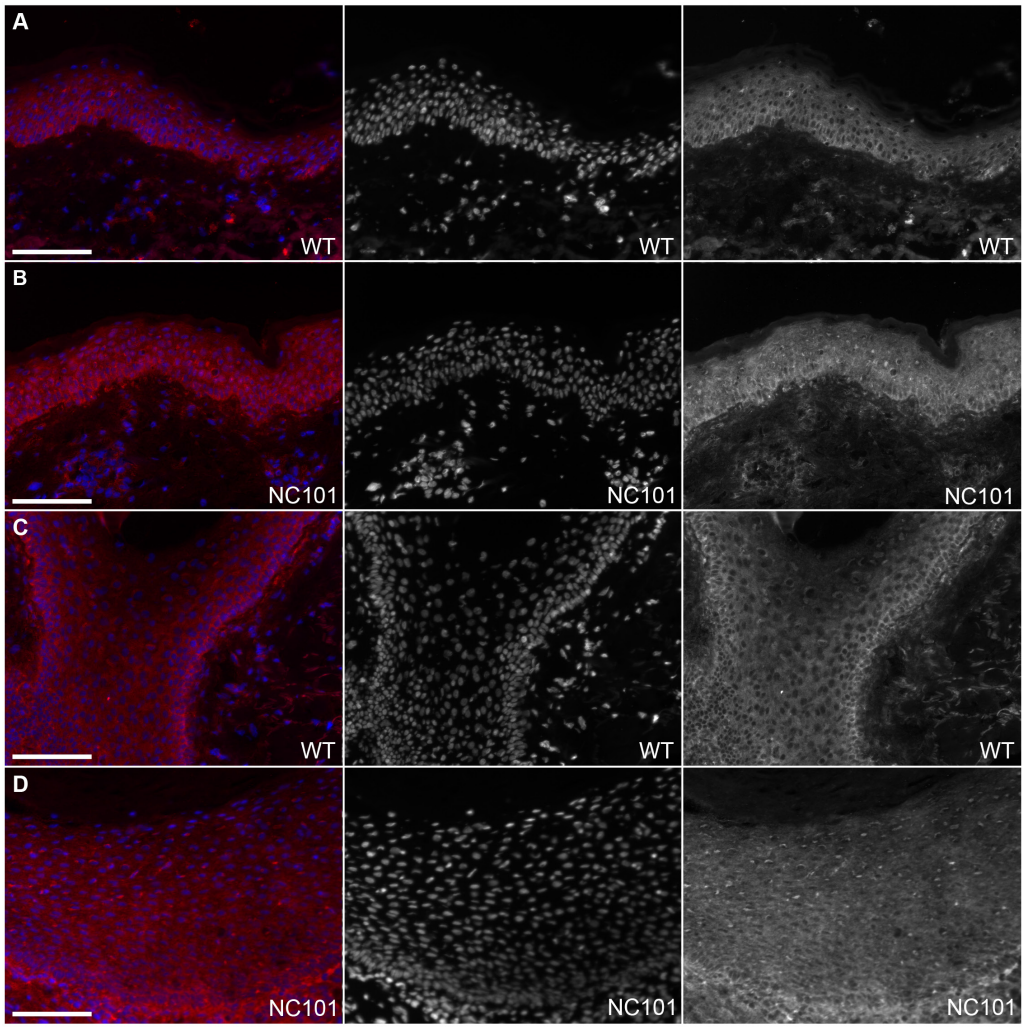

Supplemental Figure 5. NEK9 shows cytoplasmic localization in wild-type and NC epidermis. Frozen lesional NC tissue and wild-type (WT) tissue from margins of surgical excisions were fixed with 1:1 methanol:acetone at -20 C. Rabbit Anti-NEK9 antibody (Abcam; ab138488) was used at 1:250 dilution. Immunolocalization studies show that NEK9 localizes to the cytoplasm in IFE (A) and hair follicles (C) in wild-type tissue, and shows cytoplasmic localization in NC101 IFE (B) and cysts (D). Scale = 100 µm.

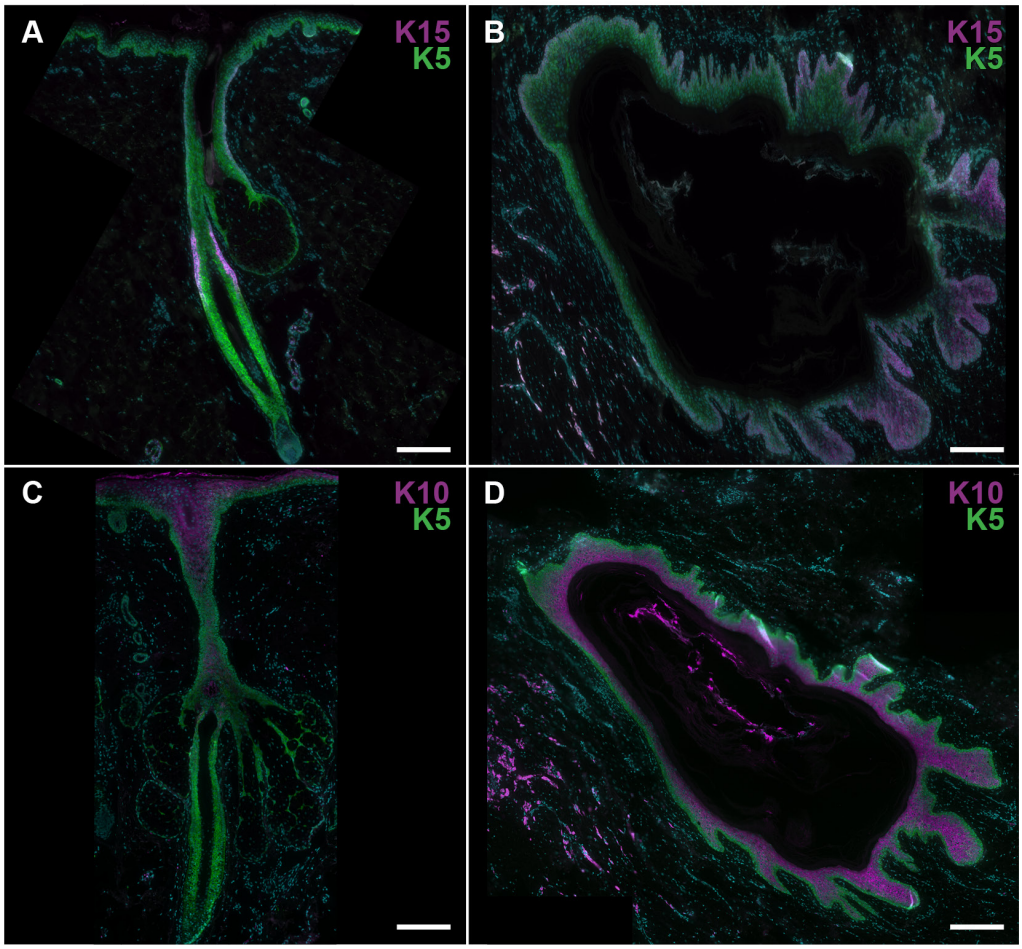

Supplemental Figure 6. Expansion of K15 localization and ectopic K10 immunolocalization in NC comedones and cysts. Stitched images of normal and NC tissue further illustrate the defect in differentiation found in NC. In normal hair follicles, K15 is found localized within the bulge region (A). However in NC, we see ectopic K15 staining of deep dermal cysts, (B). K10 is restricted to the IFE and superficial regions of the wild-type hair follicles (C), however we see suprabasal localization of K10 in NC follicles and deep dermal cysts (D). Scale = 200 μm.

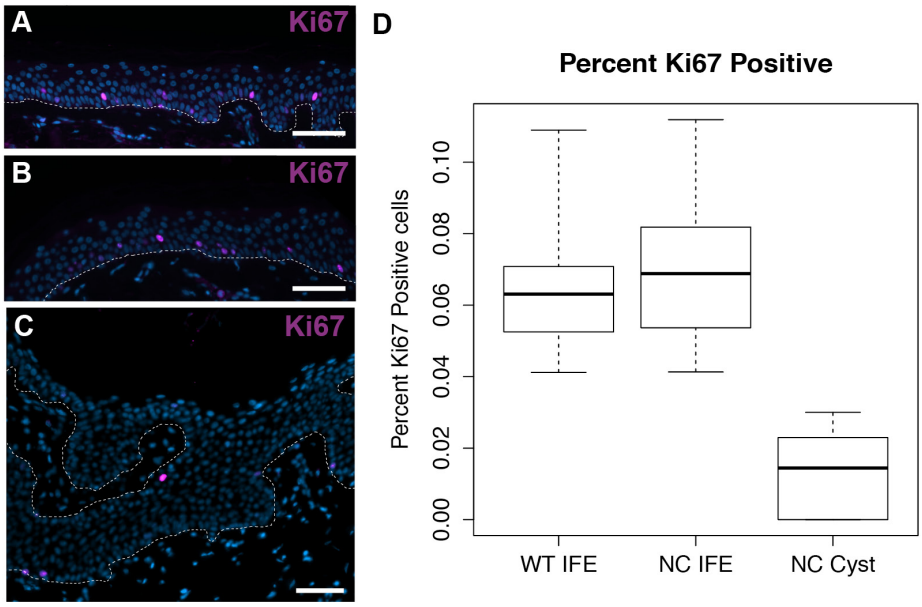

Supplemental Figure 7. Ki67 immunolocalization reveals no evidence of hyperproliferation in NC tissue. To assess proliferation within NC lesions, Ki67 (Abcam; 15580, 1:300 dilution), positive cells were counted in twenty 20x fields of view and normalized to total number of basal keratinocytes. T-tests were performed to compare the NC IFE, WT IFE, and NC cyst tissue. T-test of Ki67 staining revealed similar number of positive cells in WT IFE (A) and NC IFE (B) tissue, p-value = 0.459 (D). Cystic regions of NC tissue demonstrated fewer Ki67 positive cells than either WT or NC IFE (C,D), p-values < 10^{-8}, T-test. Scale = 50 μm.

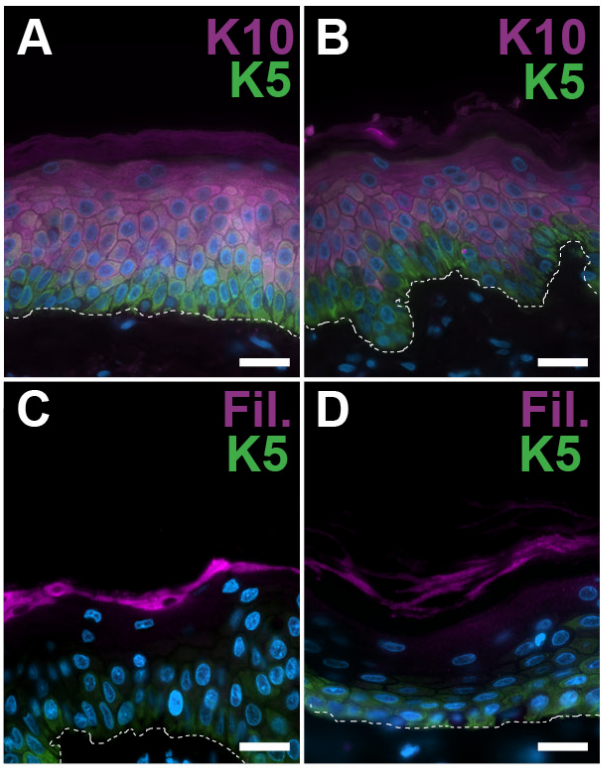

Supplemental Figure 8. NC IFE shows features of normal differentiation. Keratin 10 localizes to supra basal layers of wilt-type tissue (A) (Santa Cruz; sc-53252, 1:200 dilution) (A) and is also suprabasal in NC103 IFE (B). Similar localization of filaggrin (Abcam; ab17808, 1:400 dilution) is seen in wild-type (C) and NC103 IFE (D). Keratin 5 staining marks the basal layer of the IFE. Dermal-epidermal junction is marked by dashed white line. Scale bar = 20 μm.

Sample	Mean Coverage	Bases Covered >8x	Bases Covered >20x	Mean Read Length
NC101 Tissue	189.9x	98%	97%	74 bases
NC101 Blood	107.9x	97%	93%	74 bases
NC102 Tissue	93.4x	98%	94%	74 bases
NC102 Blood	86.9x	97%	88%	74 bases
NC103 Tissue	119.5x	97%	94%	74 bases
NC103 Blood	86.6x	97%	93%	74 bases

Supplemental Table 1. Whole exome sequencing coverage. Whole exome paired-end 74bp sequencing of tissue and blood was performed for three samples. DNA was sheared and barcoded, followed by capture with Roche EZ exome V3 capture probes. Sequencing was performed using the Illumina HiSeq 2500. Blood samples were run at 6 samples per lane, while tissue samples were run at 4 samples per lane. Sequence was aligned to hg19 using BWA-MEM. Reads were then trimmed. PCR duplicates removed using Picard and BAM files were calibrated with GATK. In all samples, >97% of coding region bases are covered >8x yielding sufficient coverage for analysis.

SSNVs Called with Filter	NC101	NC102	NC103
All Called	16	50	22
Within Exons/ Splice Sites	9	21	22
Nonsynonymous	7	13	15
> 0.1% Prevelance in ExAC	3	6	13
Fisher Test p-value > 0.1%	2*	1*	1*

Supplemental Table 2. SSNV filtering results. To identify tissue-specific mutations, a Perl script was used in tandem with MuTect. A Fisher Exact test was performed to determine non-reference read enrichment in tissue, and SSNVs with p-value greater than $1x10^{-3}$ were excluded; genome wide significance is $1.7x 10^{-6}$ after Bonferroni correction. The smallest p-values of the Fisher test for damaging SSNVs not within *Nek9* were 0.25, 0.02 and 0.12 in NC101, NC102 and NC103, respectively. To remove non-damaging SSNVs, we filtered to exclude synonymous mutations and intronic variants. SSNVs reported at greater than 1% of the population in the ExAC control database were filtered. SSNVs were then inspected on Integrative Genome Viewer (IGV) to ensure correct mapping. The remaining 4 *NEK9* mutations were not found within ExAC, 1000 Genomes and NHLBI Exome Variant Server, and dbSNP control data sets. Mutations found via WES were validated with Sanger sequencing, and confirmed via laser capture microscopy in NC101 and NC103, for which tissue was available (Figure S2). Asterisk indicates that all of these mutations were within *NEK9.*